JOURNAL OF PROPULSION AND POWER
Vol. 22, No. 4, July–August 2006

Combustion of Ammonium Dinitramide, Part 2: Combustion Mechanism

Valery P. Sinditskii,* Viacheslav Y. Egorshev,† Anton I. Levshenkov,† and Valery V. Serushkin†
Mendeleev University of Chemical Technology, 125047, Moscow, Russia

Temperature profiles in the ammonium dinitramide (ADN) combustion wave were measured in the 0.04–10 MPa pressure interval using thin tungsten-rhenium thermocouples. The data obtained suggest that the ADN decomposition reaction in the condensed zone plays a dominant role in burning at low pressures. The heat feedback from the gas to the surface appeared to be negligibly small. It has been concluded that the reaction of AN dissociation to form NH_3 and HNO_3 controls the ADN burning surface temperature. The three-zone flame structure of the ADN combustion wave has been found, and the main chemical reactions occurring in the zones have been proposed. At low pressures (below 1 MPa), the burning of ADN can be satisfactorily described by a condensed-phase combustion model with the rate-controlling reaction being the ADN decomposition in the melt. A gas-phase model with the rate-controlling reaction being HNO_3 decomposition in the first flame can be used at high pressures (above 10 MPa). In the middle pressure interval, ADN shows combustion instability caused by deficiency of heat produced in the condensed material. In this area the fast but energy-limited heat-release process in the condensed phase has to adapt itself to the slow but energy-rich heat-release process in the gas phase.

Nomenclature

A	=	preexponential factor of the leading reaction
a	=	formal order of the leading reaction
c_p	=	average specific heat of the condensed phase
E	=	activation energy of the leading reaction
k	=	rate constant
L_{dis}	=	heat of dissociation
L_m	=	heat of melting
L_v	=	heat of evaporation
m	=	mass burning rate/mass evaporation rate
n	=	pressure exponent
p	=	pressure
r_b	=	burning rate
T_a	=	temperature of the aerosol flow above the surface
T_f	=	flame temperature
T_s	=	surface temperature
T_0	=	initial temperature
T_1	=	first flame temperature
T_2	=	second flame temperature
α	=	extent of the decomposition reaction proceeds in the condensed phase
ΔH^0_{diss}	=	enthalpy of dissociation
ΔH^0_f	=	enthalpy of formation
η	=	mole fraction of nitric acid in the gas
λ	=	average thermal conductivity
μ	=	molecule weight of a salt
σ_p	=	burning-rate temperature sensitivity
χ	=	thermal diffusivity

Received 1 June 2005; revision received 15 November 2005; accepted for publication 12 November 2005.

*Professor, Department of Chemical Engineering, 9 Miusskaya Square; vps@rctu.ru.

†Associate Professor, Department of Chemical Engineering, 9 Miusskaya Square.

This paper is dedicated in memory of Professor K. K. Andreev, the founder of energetic materials research school at Mendeleev University of Chemical Technology, on the occasion of his centenary.

I. Introduction

AMMONIUM dinitramide (ADN) is being investigated intensively because it is considered an oxidizing agent potentially superior to conventional ammonium perchlorate (AP). Unquestionable advantages of ADN over AP manifest themselves in the possibility to produce more energetic propellant compositions with no HCl in the combustion products, which is very important from an ecological standpoint. A comprehensive understanding of chemical processes during combustion is essential for modeling combustion behavior of energetic materials, which can be used to predict the performance of the materials in the practical application. Investigations in this field indicate that the combustion behavior of ADN differs essentially from that of AP.[1,2] The main line of the inquiries is elucidation of mechanisms of ADN thermal decomposition and combustion. For these purposes, several investigative techniques have been used: combined spectroscopic and thermal differential scanning calorimetry (DSC) and thermal gravimetric analysis (TGA) analyses,[3] T-jump/FTIR spectroscopy with high-rate heating,[4] isothermal decomposition manometric technique,[5] DSC and thermogravimetry coupled with mass spectrometry,[6] thin-film laser pyrolysis,[7] and photolysis of ADN solutions.[8] Thermal decomposition of ADN and its ^{15}N and ^{2}H isotopes have been studied in Ref. 9. The decomposition of different forms of dinitramide, kinetics of dinitramide interaction with decomposition products, and kinetics of heat release in thermolysis of molten ADN have been studied in Refs. 10–12 by means of dynamic microcalorimeter. Several studies have been performed on ADN basic combustion characteristics[13–19] and on the interaction of ADN with fuel and potential binder materials.[15,16,20–24] Quantitative gaseous species measurements have been obtained by pyrolysis/mass spectrometry under low-pressure conditions,[25] by microprobe sampling and mass spectrometer analysis in both self-sustained combustion,[26,27] and CO_2 laser-induced deflagration.[13,19]

Measurements of thermal structure of the combustion wave provide critical data for understanding combustion mechanism. A series of recent works[13–16,18,19,22,26] deal with temperature measurements in the ADN combustion wave, often accompanied by quite different interpretations of experimental results. This work presents a detailed analysis of experimental temperature profiles in the ADN combustion waves resulting in a relative mechanism of ADN combustion.

II. Experimental

Sample preparation: ADN was used for burning-rate experiments as obtained by a technique given in Ref. 28 followed by

recrystallization from 95% water ethanol. The only stated impurity was about 0.4% by weight of ammonium nitrate.

To obtain ADN containing 0.2% of paraffin, thoroughly grinded ADN (particle size less than 60 μm) was treated with a solution of the required amount of paraffin in pentane or chloroform and dried in air with stirring followed by storage under vacuum.

Burning-rate measurements: Burning-rate measurements were carried out in a constant-pressure window bomb of 1.5-liter volume. The pressure range studied was 0.1–36 MPa. Measurements in the subatmospheric region were conducted in a vacuum chamber of 40-liter volume. A slit camera was used to determine the character of the combustion process as well as the burning-rate values.

Temperature measurements: Temperature profiles in the combustion wave of ADN were measured using Π- and Γ-shaped thermocouples. The thermocouples were welded from 25- or 50-μm-diam tungsten—5% rhenium and tungsten—20% rhenium wires and rolled in bands to obtain 7- or 20-μm bead size. The thermocouples were embedded in ADN pressed into quartz tubes with internal diameter of 8.5 mm. The mean density of the samples was 1.54 g/cm^3, and 20-μm-thick thermocouples were used only in measuring the maximum flame temperature.

Γ-Shaped 7-μm-thick thermocouples fixed vertically in the centers of the quartz tubes with the help of thin quartz binary capillaries were employed to measure temperature profiles of liquefied ADN. First the tube was filled with crystalline ADN and then slowly heated up to approximately 100°C so that all of the crystals were melted. As soon as that occurred, the test was run.

Temperature measurements were conducted at 0.5, 1.1, 2.1, 4.1, and 10 MPa for crystalline ADN, at 0.04, 0.06, 0.1, and 0.5 MPa for ADN with 0.2% of paraffin, and at 0.1 MPa for molten ADN. In all cases the burning rate was measured simultaneously with recording temperature profiles.

III. Results and Discussion

A. Temperature Measurements in the ADN Combustion Wave

Pure crystalline ADN is known to be incapable of sustained burning at room temperature and atmospheric pressure. ADN can burn at atmospheric pressure only upon being liquefied and heated to about 100°C. The burning rate was measured to be 8.4–9.1 mm/s. It is also known that even minor amounts of organic admixtures have a strong effect on ADN burning behavior, extending considerably the low-pressure limit of deflagration to the vacuum area.[14,22] For example, an addition of as small an amount of paraffin as 0.2% to crystalline ADN appeared to extend the low-pressure limit of ADN sustained combustion from 0.2 to 0.02 MPa. Therefore, it can be deduced that those studies which describe combustion of ADN at atmospheric and subatmospheric pressures deal with impure ADN.

At atmospheric and subatmospheric pressures paraffin-doped ADN burns without any luminous emission, forming copious white vapors, which condense as a fine white powder inside the tube and at cold surfaces of the bomb.

In the subatmospheric pressure region (at 0.04 and 0.06 MPa), the temperature profiles for paraffin-doped ADN are typical of flameless combustion: a sharp temperature increase in the condensed zone is followed by the gas zone of practically constant temperature, that is, with practically zero temperature gradient above the burning surface. This temperature remains almost constant over all of the length studied (~6 mm) and is equal to 553–563 K and 583–603 K, at 0.04 and 0.06 MPa, respectively (Fig. 1).

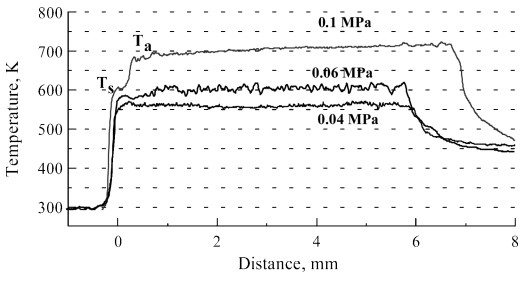

Fig. 1 Temperature profiles for paraffin-doped ADN at pressure of 0.04, 0.06, and 0.1 MPa.

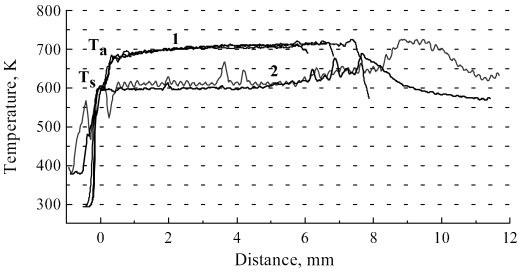

Fig. 2 Comparison of temperature profiles for molten (2) and paraffin-doped (1) ADN at atmospheric pressure.

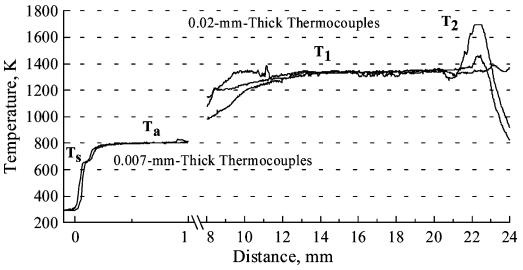

Fig. 3 Temperature profiles of ADN at 0.5 MPa. T_s is surface temperature, and T_a is temperature of the aerosol flow above the surface. T_1 and T_2 are the first and the second flame temperatures, respectively.

At 0.1 MPa, temperature measurements were carried out with molten ADN and paraffin-doped ADN, both capable of sustained burning at this pressure. Surface temperatures T_s for both materials were determined to be within the range 593–608 K (Fig. 2). Invariability of the surface temperature with changing initial temperature is consistent with a hypothesis that the temperature at the ADN burning surface is controlled by a thermodynamic transition such as boiling or dissociation. Another important feature of the ADN combustion profile, which appears at 0.1 MPa, consists of the temperature above the burning surface T_a of paraffin-doped ADN rises gradually to ~700 K and then remains practically constant over a distance above the surface as long as 18 mm (in the case of using 20-μm-thick thermocouples). For combustion of liquefied ADN, temperature above the burning surface increases very slowly starting from the surface temperature and showing sporadic splashes to 650–700 K.

Close but slightly lower values of the surface temperature at 0.1 MPa were observed by other researchers during laser-induced regression of pure ADN (570–580 K)[13,19] and in sustained combustion of impure ADN (588 K,[26] 560 K,[16] and 533 K[18]). The temperature above the burning surface was measured to be also very close to our results (683 K,[13,19] 700 K,[26] 720 K,[16] and 753 K[18]).

The temperature gradient above the surface and the heat feedback from the gas to the condensed phase were calculated in Refs. 16 and 18 based on measured T_s and T_a. However, as follows from the detailed temperature distribution at 0.1 MPa shown in Fig. 2, there exists a clear region above the surface, between T_s and T_a, in which the temperature gradient is virtually equal to zero. Therefore, it is safe to assume that there is no heat feedback from the gas phase, at least at low pressures.

The ADN surface temperature is believed to increase to 655–675 K as the pressure is increased to 0.5 MPa (Fig. 3). Temperature T_a reaches 805–820 K just above the surface (~1 mm). In the case of finishing combustion or spontaneous extinguishing, the profiles demonstrate spikes of the temperature immediately upon ceasing combustion. These temperature spikes were presumed to be caused by entering a remote first flame into the tube and reaching the thermocouple as soon as the gas flow from the surface stops. Indeed, tests with long strands and 20-μm-thick thermocouples showed an increase in temperature to 975–1075 K at a distance of 7–8 mm followed by a sharp growth to 1325–1350 K (T_1). Interestingly, in some tests with long strands there also appeared temperature spikes at the end of burning.

Paraffin-doped ADN showed similar profiles at this pressure, except that the intensive temperature rise in the gas phase to T_1 began with 3–4 mm above surface rather than with 8–10 mm for pure ADN.

At 1.1 MPa and higher pressures, the position of the surface temperature at profiles is difficult to determine (Fig. 4). A slight break in the profiles can be observed at 710–755 K. The temperature T_a just above the surface (at 0.2–0.3 mm) was determined to be 825–855 K followed by its progressive increase to 1225–1285 K (T_1) at a distance of 2–4 mm. A further slight increase in the gas-phase temperature was revealed by tests with long strands, achieving 1465–1475 K at a high of 12 mm above the surface.

Temperature measurements at 2.1 and 4.1 MPa were carried out only with the help of 7-μm-thick thermocouples embedded in short samples (Fig. 4). At 4.1 MPa the surface temperature was no longer detectable even with 7-μm-thick thermocouples owing to too high burning rate of ADN. At 2.1 MPa the temperature above the surface T_a was determined to be 845–895 K followed by its sharp increase to 1325–1375 K (T_1) at a distance of 1–2 mm. At 4.1 MPa the temperature rises ~850 K above the surface to 1350–1400 K at a distance of 0.8–1 mm and then remains practically unchanged up to 4 mm distance. In spite of narrow flame zones, there are still breaks in the profiles at ~850 K, which correspond to T_a.

At all of these pressures, the maximum measured temperatures of ADN combustion did not correspond to the calculated adiabatic one (about 2050 K). The high-temperature second flame T_2 appeared at 10 MPa at a distance as small as 0.2 mm off the surface. However, at high pressures and temperatures the tungsten thermocouples tend to vigorous oxidation in the oxidizing surroundings, resulting in burn out and showing too high temperature. The profiles at 10 MPa reveal also characteristic brakes at 1375–1575 K, corresponding to T_1. Because of high burning rates exceeding the admissible level for the thermocouples used, the real temperature gradient above the surface could not be derived from the profiles at high pressures.

For combustion of impure ADN, the high-temperature flame T_2 appears at a closer distance to the surface. It was observed at ~1 mm standoff distance at pressure of 2 MPa (Ref. 16).

All of the data from the temperature measurements are collected in Fig. 5. The dashed line is the pressure dependence of the dissociation temperature of ammonium nitrate (AN),[29] which proves to be in a good agreement with the surface temperatures. Also presented here are data of Fetherolf and Litzinger[13,19] on temperature measurements in laser-induced combustion of ADN at 1, 3, and 5 atm. As seen in Fig. 5, the results of our work and those obtained in Refs. 13 and 19 are in a good agreement. Somewhat understated temperatures of the second zone measured at 2.1 and 4.1 MPa can result from the fact that we used short strands within which the thermocouple was only able to measure the temperature of the beginning of the zone, rather than its maximum steady temperature.

The surface temperatures measured in Ref. 16 at 0.066, 0.1, 2, and 6 MPa are somewhat less, and those in Ref. 18 at 0.1, 0.7, 2, 4, and 6 MPa are considerably less than our data. ADN has extended flame zones that facilitate finding of characteristic temperatures. In this connection the difference between our data and data of Refs. 16 and 18 is thought to be caused by different approaches to identify the surface temperature on the profiles rather than measurement errors. The reliability of surface temperatures found in Ref. 16 on profiles at pressures above 2 MPa is questionable because of too high burning rates and, as a consequence, very narrow combustion zones comparable with thermocouple thickness.

A characteristic of the combustion behavior of ADN is not only unusually extended flame zones—that has been also observed for combustion of ADN/binder sandwiches[20]—but multistep heat release during the process as well. The extension of the ADN flame zones depends on pressure (Table 1).

Analysis of ADN temperature profiles at different pressures allows three distinctive zones to be distinguished in the ADN flame (Fig. 6). Just above the surface, the temperature is constant at a value equal to the surface temperature for some time and then increases moderately in a stepwise manner. This flame zone is easily observed for the combustion of ADN + 0.2% paraffin at atmospheric pressures (Fig. 1).

The magnitude of the temperature step between T_s and T_a is about 120–145 K. As the pressure increases, the zone tends to contract rapidly. The temperature of ADN surface is clearly discernible in profiles at low pressures, but it is no longer detectable above 2 MPa. At 0.5 MPa, there appears the first flame, in which the temperature rises to 1325–1475 K (at 0.5–4 MPa). In any event, the maximum

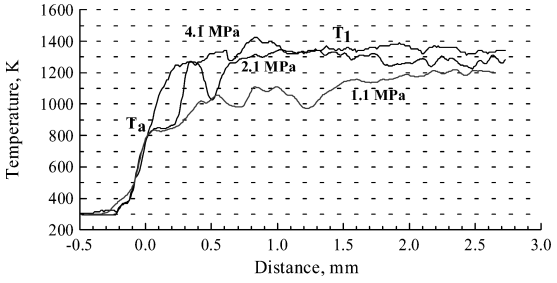

Fig. 4 Temperature profiles for pure ADN at pressures of 1.1, 2.1, and 4.1 MPa.

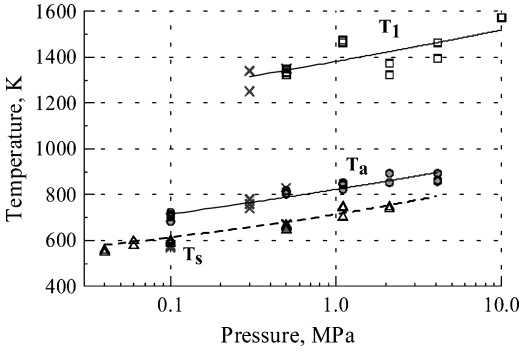

Fig. 5 Effect of pressure on the ADN surface and flame temperature: surface temperature (△), temperature of the aerosol zone (○), temperature of first flame (□), and data of Fetherolf and Litzinger (×).[13] The - - - - is the dissociation temperature of ammonium nitrate.[29]

Table 1 Surface temperature T_s, aerosol zone temperature T_a, and standoff distances of ADN flame zones

			Standoff distances, mm	
Pressure, MPa	T_s, K	T_a, K	First flame	Second flame
0.04	558 ± 7	——[a]	——	——
0.06	593 ± 14	——[a]	——	——
0.1	602 ± 6	706 ± 15	——	——
0.5	663 ± 10	810 ± 8	7–8	>25
1.1	736 ± 25	842 ± 13	1–2	>16
2.1	748 ± 25	866 ± 25	0.5–1	12
4.1	——	871 ± 20	0.5–1	>4
10.0	——	——	——	<0.2

[a]Is not observed over a distance ~6 mm above the surface.

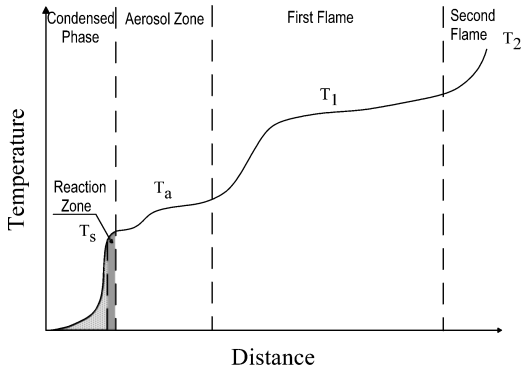

Fig. 6 ADN multistep conversion in the combustion wave. T_s is surface temperature, T_a is temperature of the aerosol flow above the surface. T_1 and T_2 are the first and the second flame temperatures, respectively.

combustion temperature representing full heat release is not still attained at moderate pressures. Temperature spikes observed at times at the end of combustion do suggest the presence of one more high-temperature zone, which stands far off the surface.

Temperatures T_a and T_1 in Ref. 18 are considered as belonging to one flame, in which the temperature grows from 725 K at 0.1 MPa to 1475 K at 4 MPa. The results of our work show that the temperature zone T_a exists concurrently with the zone T_1 at pressures up to 4 MPa.

By applying one-dimensional conductive heat-transfer analysis, the thermal diffusivity χ of condensed ADN can be evaluated from the temperature profiles. For the nonreactive region, a plot of $\ell n(T - T_0)$ vs distance yields a straight line with a slope of r_b/χ. At temperatures below 350 K, the slope of the line yields a thermal diffusivity $(1.78 \pm 0.3) \cdot 10^{-7}\ \mathrm{m^2 \cdot s^{-1}}$, which is in good agreement with data of D. Hansen-Parr $(1.87 \cdot 10^{-7}\ \mathrm{m^2 \cdot s^{-1}})$ obtained by another technique (data cited in Ref. 7). At temperatures above 350 K for pressures 0.04 and 0.06 MPa, and above 400 K for pressure 0.1 MPa, there is observed an increase in the slope associated with the existence of exothermic reactions in the melt.

B. Possible Combustion Mechanism of ADN

The decomposition of ionic salts, such as AN and AP, is initiated by proton transfer and then is determined by decomposition of the formed acid and following reactions with NH_3.[30] This mechanism is stipulated by a big difference in the decomposition rates between the anion and acid, with a high decomposition rate being provided by even a very low equilibrium concentration of acid. However, in the case of dinitramide there is a small difference in the reaction rates of the anion and acid, resulting in the fact that the both species are of significant importance in ADN thermal decomposition.[10–12]

Flameless burning at low pressures and the lack of heat feedback from the gas phase observed in temperature profiles all are indicative of domination of the condensed phase in ADN combustion. The good agreement between measured surface temperatures and ammonium-nitrate dissociation temperatures gives grounds to consider that the unique decomposition reaction of ADN to form condensed AN and gaseous N_2O occurs at the surface:

$$NH_4N(NO_2)_2(l) \rightarrow NH_4NO_3(l) + N_2O + 33\ \mathrm{kcal/mole} \qquad (1)$$

The ionic mechanism involving formation of ammonium nitrate has been put forward as one of ADN decomposition pathways in Ref. 6, based on the absence of NH_3 at early stages of the thermolysis. Monomolecular rearrangement of ADN and other dinitramide salts with strong bases is presented in Refs. 31 and 32. The ionic mechanism has been also considered in Ref. 9 as a dominant decomposition mode below 160°C.

During combustion of many onium salts, the surface temperature is governed by the dissociation reaction of a salt, that is, by splitting the donor-acceptor bonds between base and acid followed by their volatilization into the gas phase. The dissociation process is similar to boiling of molecular substances such as water, that is, the phase-change process of the first kind. The dissociation is characterized by the enthalpy of dissociation, which in a sense is equal to enthalpy of evaporation for molecular substances. The dissociation temperature (temperature at which the vapor pressure above a salt is equal to ambient pressure) of ADN is bound to be higher than that of AN as dinitramidic acid is stronger (pKa −5.62 (Ref. 33) or −4.85 (Ref. 10)) than nitric acid (pKa −1.64). It is proposed, therefore, in Ref. 14 that it is ammonium nitrate formed by the reaction (1), which dissociates from the ADN burning surface, thus controlling the surface temperature:

$$NH_4NO_3(l) \rightarrow HNO_3(g) + NH_3(g) \qquad (2)$$

The supporting evidence was obtained from thermocouple-aided measurements in the combustion wave and analysis of the condensed combustion products.

Coincident with dissociation, the carryover of small droplets of molten substance to the gas phase takes place, which has been observed in many studies, but usually prescribed to AN only. In Refs. 14 and 16, it has been found that condensed residue after ADN combustion at low pressures consists of an AN and ADN mixture, with the ADN content increased as the pressure decreases. At atmospheric pressure, the ADN content of the residue after combustion of ADN +0.2% paraffin has been determined to be around 6% (Ref. 14). Dispersion of the molten surface layer is typical of materials that burn at the expense of condensed-phase reactions.[34,35] This is caused by breaking the molten surface layer by blowing off gases, on the one hand, and physical impossibility of full evaporation at the expense of the condensed-phase heat release, on the other hand. In the absence of heat feedback from the gas, there is no opportunity for the substance to be evaporated except for the surface-layer physical and thermal inhomogeneity: foaming, local overheating, and mixing the melt by gaseous decomposition products.

With growing pressure, flame distances decrease, and decomposition completeness increases, resulting in the disappearance of condensed combustion products. However, as indicated by thermocouple measurements, the aerosol zone containing molten AN and ADN still exists up to pressure of 2 MPa at least. The aerosol zone above the surface is likely to exist at higher pressures also. The temperature T_a is recognizable at pressure of 4.1 MPa, at which the burning rate is so high that a thermocouple will be able to record the break on the profile if the temperature zone T_a is large enough.

The presence of ADN droplets in the aerosol zone is evidenced by a small temperature rise in the first flame zone. This step is easily observed on the temperature profile at atmospheric pressure (see Fig. 1) and sets in as soon as condensed AN dies out from the flow. In doing so, the temperature of the aerosol flow grows up to the dissociation temperature of ADN still remaining in the flow:

$$NH_4N(NO_2)_2(l) \rightarrow HN(NO_2)_2(g) + NH_3(g) \qquad (3)$$

The dissociation temperature of ADN is bound to be higher than that of AN. At atmospheric pressure, this temperature is unchanged through the profile because ADN droplets are present all of the way to completion of combustion. For combustion of liquefied ADN at atmospheric pressure, the temperature above the surface remains equal to the temperature of AN dissociation over a large distance because of much higher velocity of the gas flow.

The variation of surface and first flame zone temperatures with pressure is presented in Fig. 7. Also presented is the dissociation pressure–temperature dependence for ammonium perchlorate[36,37] and nitrate.[29] The surface temperatures of ADN appear to be very close to the dissociation temperature of AN. The temperatures of the first flame zone T_a lay between the NH_4NO_3 and NH_4ClO_4 dissociation temperatures. The resulting line for the temperatures of the first flame zone T_a can be expressed by the following equation:

$$\ell n\, P = -11352.9/T + 15.9$$

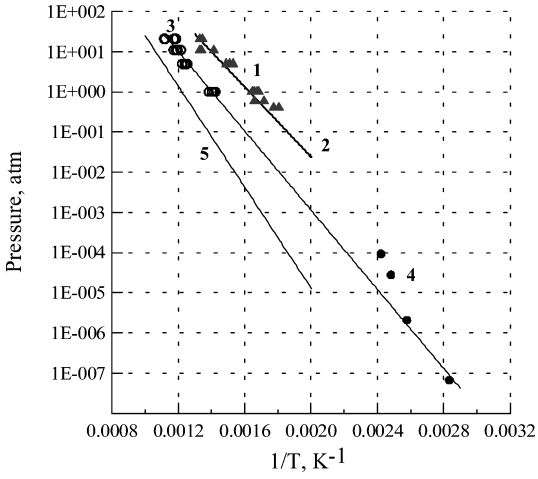

Fig. 7 Vapor pressure as a function of reciprocal temperature for ammonium salts: 1 (△), ADN surface temperature; 2 (—), vapor pressure of AN[29]; 3 (○ and —), temperature of the aerosol zone T_a; 4 (●), vapor pressure of ADN[36]; and 5 (—), vapor pressure of AP.[37]

Because the maximum achievable temperature to which an onium salt can be heated up is the temperature of its dissociation, the slope of the line constructed in $\ln P$ vs reciprocal temperature coordinates with taking into account two gaseous molecules formed at salt dissociation will yield the enthalpy of the salt dissociation ΔH^0_{diss}. The experimental data for ADN plotted in the above coordinates give $\Delta H^0_{\text{diss}} = 2R \cdot 11.35 = 45.1$ kcal/mole. A rough estimate of a possible error yields 2 or 3 kcal. A calculation based on the experimental ΔH^0_f of ADN (−32 kcal/mole)[1] and NH_3 (−10.92), (see Ref. 38) calculated ΔH^0_f of gaseous dinitraminic acid (24.9 kcal/mole)[39] and enthalpy of ADN melting taken as 3.4 kcal/mole, gives ΔH^0_{diss} of ADN as 44.4 kcal/mole, which is in good agreement with our result. Politzer et al.[40] presented new calculated values of heat of formation of $HN(NO_2)_2$ in the gas phase and heat of ADN dissociation, 19 and 44 kcal/mole, respectively. These data are also in good agreement with ours.

In Ref. 39, it is suggested on the basis of calculated enthalpies of formation of ADN and dinitramide that ADN gasification includes evaporation to produce a gaseous "molecular complex" $NH_3 \cdot HN(NO_2)_2$ with enthalpy of formation of 3.2 kcal/mole followed by its dissociation to form ammonia and dinitramide, with the heat of dissociation reaction of 12–14 kcal/mole. Such a gasification process has not ever been considered earlier, not to mention experimental confirmations. From our point of view, the authors of Ref. 39 used ideas appropriate for salts like LiCl, but unacceptable for onium salts. In the latter case, vaporous material consists of almost wholly gaseous base and acid, with the portion of associate being negligible.[41] Our results are indicative of this also. If ADN is assumed to evaporate to produce the molecular complex $NH_3 \cdot HN(NO_2)_2$, as suggested in Ref. 39, the slope of the line constructed in ADN vapor pressure vs reciprocal temperature coordinates yields the heat of vaporization of 22.5 kcal/mole, which differs strongly from a value of 35.2 kcal/mole calculated from enthalpy of formation the molecular complex.[39]

Ermolin[42] carried out a numerical modeling of ADN pyrolysis in $373 \div 920$ K temperature interval and showed that the model described was in a good agreement with experimental data of Ref. 38 if only the dissociative mechanism were assumed.

One more confirmation of ADN dissociation at the first flame zone can be obtained from comparison of the aerosol flow temperature T_a and ADN vapor pressures taken from Ref. 36. The authors of this work follow the idea that ADN evaporates from the burning surface as the molecular complex and gives the enthalpy of evaporation of 37.1 kcal/mole. However, the fitting line through the points of T_a in Fig. 7 extrapolated into the low-temperature area just passes through the data points of Ref. 42 at 80 and 115°C. The data points at 130 and 140°C lie above the line, which can be reasonably explained by increasing ADN decomposition at elevated temperatures (5–8% even with no autocatalysis taken into account).

As long as AN droplets are present in the flow, the temperature of the flow is kept constant because of continued dissociation of AN into NH_3 and HNO_3. Because the dissociation enthalpy is about 39–40 kcal/mole,[29] it is apparent that the heat evolved in the reaction (1), 33 kcal/mole, is insufficient for warming up, melting, and dissociation of the condensed substance. Therefore, some other exothermic reactions are to be considered as proceeding simultaneously with reaction (1). Quantitative measurements of gaseous species by microprobe sampling[13] and T-jump/FTIR technique[4] at atmospheric pressure have demonstrated that the amount of water is comparable to the amount of N_2O at some distance off the ADN sample surface. The occurrence of water at this early stage can hardly be a result of AN thermolysis because the rate of AN decomposition is 10^7–10^8 times less than the decomposition rate of the dinitramide salt. Based on the ADN thermolysis pathways proposed in Refs. 3–5 and 9–12, it is possible to assume that the other ADN decomposition channel in the melt is the decomposition reaction of extremely unstable dinitramidic acid, which is formed in both the gas and condensed phases according to the reactions (3) and (4):

$$NH_4N(NO_2)_2\,(l) \Leftrightarrow HN(NO_2)_2(l) + NH_3(l) \tag{4}$$

$$HN(NO_2)_2(g/l) \rightarrow NO_2 + HNNO_2 \rightarrow OH + N_2O \tag{5}$$

The following interaction between radicals formed by reaction (5) with gaseous NH_3 or NH_3 dissolved in the melt produces more than 50 kcal/mole,[12] as a result of formation of gaseous water, nitrogen, nitrogen oxides, and nitric acid.

$$NO_2/OH + NH_3 \rightarrow H_2O, N_2, NO, N_2O \tag{6}$$

It was suggested in Ref. 6 that the second path also follows an ionic mechanism involving formation of intermediate ammonium nitrite followed by its exothermic decomposition to give nitrogen oxide and water:

$$NH_4N(NO_2)_2(l) \rightarrow NH_4NNO_2(l) + NO_2 \rightarrow NH_4NO_2\,(l) + 2NO \rightarrow$$

$$\rightarrow 2H_2O + 2NO + N_2 + 41\ \text{kcal/mole} \tag{7}$$

The dissociation temperature of ammonium nitrite is lower than that of the other ammonium salts, ADN and AN. If ammonium nitrite had substantially existed at the burning surface, the surface temperature would have been controlled by its dissociation reaction; that was not the case according to the data of thermocouple measurements.

As soon as AN droplets die out from the aerosol flow, the temperature in the flow changes stepwise from the AN dissociation temperature to the ADN one. Disappearance of AN from the aerosol flow is connected with the fact that all heat released in the exothermic reactions (1) and (6) in the molten aerosol particles can now be almost totally consumed to dissociate AN and ADN (reactions 2 and 3), without the need to preheat and melt the substance. As a result, temperature of the flow increases and becomes higher than the AN dissociation temperature, with the ADN being the only condensed substance left in the aerosol flow. Now the reaction of ADN dissociation starts to control the temperature of the flow.

Once ADN droplets have dissociated, the temperature increases drastically to form the first flame. This flame includes reactions of oxidation of ammonia by nitric acid decomposition products (OH, NO_2) nearly to full consumption of it. The temperature of the zone, however, does not correspond to the full heat release owing to N_2O and NO remaining partially unreacted in the flame. The combustion reaction reaches its total completion only in the second flame, which was practically observed at 10 MPa, while it could be observed at lower pressures also at higher standoff distances (at 12 mm distance off the surface at 2.1 MPa). At 4.1 MPa the second flame did not appear at a distance at least 4 mm off the surface.

To summarize the preceding hypothesis, a schematic of the ADN combustion wave structure is presented in Fig. 8. Here, the ADN gas flame (from the chemical standpoint) can be visualized as the flame of AN diluted with N_2O, NO, N_2, and water. In both the condensed phase and the aerosol zone, two competitive heat-generating processes take place: ionic (reaction 1) and dissociative (reactions 3, 4, 5) followed by interaction between the radicals formed in the course of the reaction (5) with gaseous or dissolved in the melt NH_3. Analysis of the condensed products of ADN combustion at atmospheric pressure shows that the degree of conversion of ADN to AN is about 60% (Ref. 43). As pressure increases, this portion slightly

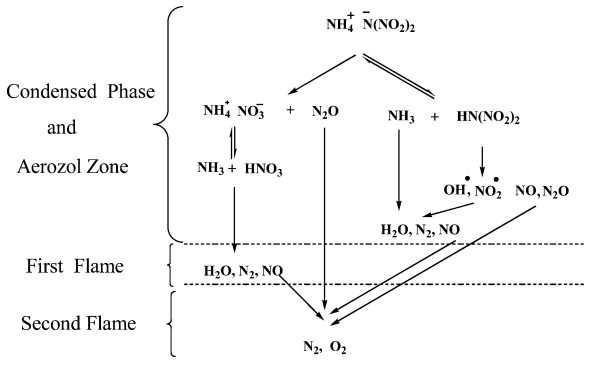

Fig. 8 Schematic of ADN flame structure.

decreases but still remains considerable. In experiments with laser-induced regression of ADN,[19] when the laser heat flux supported the ADN dissociation reaction, as much as 0.15 mole fraction of solid AN was found to be formed at atmospheric pressure that corresponded to about 50% degree of conversion of ADN to AN.

The lack of heat flux from the gas at least up to 4 MPa allows considering the condensed-phase chemistry as determining ADN combustion at low pressures. Rate constants of the dominant combustion reaction of ADN in the pressure range of 0.02–1 MPa can be obtained from Zeldovich expression[44] for the burning rate:

$$m = \sqrt{\frac{2\rho^2 \chi Q}{c_p (T_s - T_0 + L_m/c_p)^2} \left(\frac{RT_s^2}{E}\right) \cdot A \cdot e^{-E/RT_s}}$$

based on a dominant role of the condensed-phase chemistry and taking the surface temperature T_s as the AN dissociation one. The average specific heat c_p was taken as 0.49 cal/g · K, thermal conductivity of the condensed phase λ as 0.00193 cal/cm · s · K, heat of reaction Q as 400 cal/g, and the heat of melting L_m as 3.4 kcal/mole.

As seen in Fig. 9, the results derived from the combustion model, $k = 2.34 \cdot 10^{16} \cdot \exp(-39{,}000/RT)$ s^{-1}, are in a satisfactory agreement with the ADN decomposition kinetics found by different ways: from dinitramide-anion and ammonium-cation disappearance rates,[9] $k = 8.8 \cdot 10^{16} \cdot \exp(-39{,}900/RT)$ and $k = 3.6 \cdot 10^{15} \cdot \exp(-37{,}800/RT)$, and from rates of formation of gaseous decomposition products, $k = 10^{14.4} \cdot \exp(-35{,}500/RT)$[5] and $k = 2.5 \cdot 10^{15} \cdot \exp(-35{,}300/RT)$, s^{-1}.[9] All of the data can be described fairly well in the temperature interval of 370–977 K by a general line $k = 1.46 \cdot 10^{16} \cdot \exp(-38{,}500/RT)$.

According to the condensed-phase combustion model, the pressure exponent for the burning rate vs pressure dependence is defined by the activation energy of the leading reaction and the heat of a phase-change process (evaporation/dissociation), which controls the surface temperature:

$$n = E/2L_v$$

In the case of salt dissociation, when two molecules of gaseous products are produced from one molecule of the salt, the enthalpy of salt dissociation should be used instead of $2L_v$. Using the activation energy 38.5 kcal/mole and enthalpy of AN dissociation (39.9 kcal/mole), one can calculate the pressure exponent $38.5/39.9 = 0.965$. The calculated value n is close to the experimental one equal to 0.96 observed in combustion of paraffin-doped ADN in the pressure interval of 0.02–1 MPa. Experimental values n observed in combustion of crystalline ADN in the pressure range of 0.2–4 MPa are significantly less (0.46–0.6), because at these pressures the ADN burning rate vs pressure curve assumes the form of a saturated line because of changing of combustion mechanism.

It follows from the condensed-phase model that the burning-rate temperature sensitivity $\sigma_p = \partial \ln m/\partial T_0$ depends only on the surface temperature (i.e., AN dissociation temperature), and grows with pressure:

$$\sigma_p = 1/(T_s - T_0 + L_m/c_p)$$

As is shown in Ref. 43, the experimental values of σ are very close to the calculated results at 0.1 MPa, at which ADN samples demonstrated stable combustion. In the interval of 0.3–6 MPa, the temperature sensitivity begins to grow sharply with pressure, and the experimental values are considerably higher than theoretical ones. Large magnitudes of the temperature sensitivity in this pressure region are indicative of the thermal instability of combustion.

Hence, at low pressures, ADN burning rates (Fig. 10), pressure exponent, and burning-rate temperature sensitivity can be well described by the condensed-phase combustion model.

Data of temperature measurements allow attempting an explanation of ADN combustion instability observed at 1–10 MPa. Temperature profiles clearly indicate that, at least up to 4 MPa, there is a region between the surface and first flame in which the temperature gradient is close to zero. In the lack of any heat flux from the gas, the condensed phase can be heated up only at the expense of condensed-phase reactions. The total decomposition of ADN in the melt was shown in Ref. 12 to produce about 50 kcal/mole (~400 cal/g). The DSC traces of neat ADN indicated the major exotherm of 406 cal/g (Ref. 9). If the reactions proceeded completely in the condensed phase, the maximum temperature would reach about 950–1030 K. However, the heat is partly consumed to dissociate AN, making the maximum temperature less. A comparison between heat of ADN decomposition in the condensed phase and heat required to heat the condensed phase to the surface temperature, $Q_{\text{need}} = c_p(T_s - T_0) + L_m$, is presented in Fig. 11. As illustrated in Fig. 11, the heat disbalance during ADN combustion begins at 2 MPa. The temperatures of 725–775 K and 840–890 K (Table 1) are respectively the maximum ones, developed in the condensed material, and temperatures above the surface T_a. These values are less than just-mentioned maximum temperature, which is conditioned with that part of heat is consumed for salt dissociation. The extent α to which the decomposition reaction proceeds in the condensed phase can be easily estimated from the following equation:

$$\alpha = [0.1\chi \cdot k(T_s)]/r_b^2$$

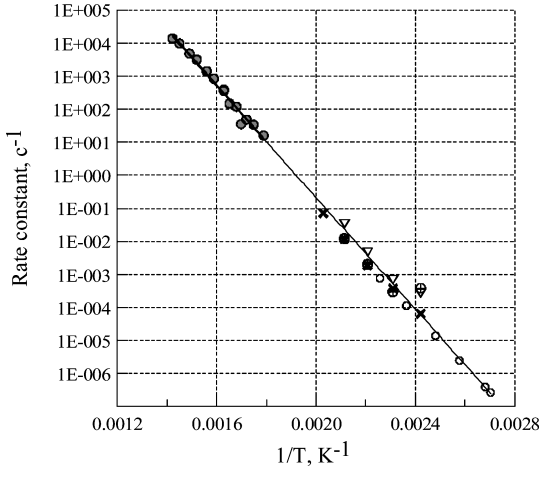

Fig. 9 Rate constants vs reciprocal temperature for the leading reaction in ADN combustion (●) and the kinetics of the ADN decomposition found from dinitramide-anion and ammonium-cation disappearance rates (△ and ⊖) and from rates of formation of gaseous decomposition products (○[5] and ×[9]). Line is drawn through all of the data.

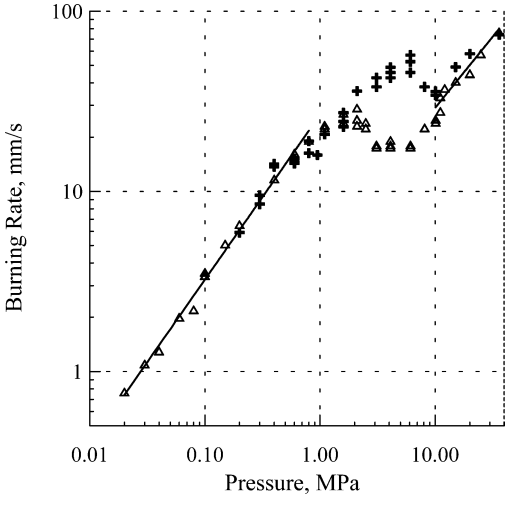

Fig. 10 Comparison between experimental and calculated (—) burning rates of pure ADN (+) and ADN with 0.2% paraffin (△) assuming condensed-phase (below 1 MPa) and gas-phase (above 10 MPa) leading reactions.

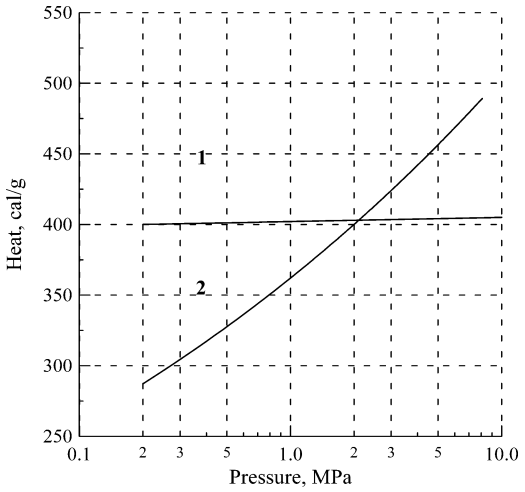

Fig. 11 Comparison between heat of ADN decomposition in the condensed phase (1) and heat required for warming up the condensed phase to the surface temperature (2).

Assuming the reaction layer is one-tenth as long as the preheated layer and using rate constants of ADN decomposition at corresponding surface temperatures, the extent to which ADN could decompose in the condensed phase increased from 50% to 80–90% with pressure increasing from 0.04 to 1 MPa. The real heat release in the condensed phase, therefore, will be less than 406 cal/g, and the heat inbalance during ADN combustion can set in even at 1 MPa. At this pressure, either a change in the combustion mechanism or initiation of the combustion instability should be expected to happen.

The following course of events can be proposed to take place as pressure grows. Increasing temperature of ADN dissociation results in the growing deficiency of heat required to warm up and evaporate the condensed material. Further heat supply could be provided by the high-temperature gas flame T_1, but it stands too far from the surface by virtue of kinetic reasons. Because of the lack of heat in the surface layer, the combustion process becomes unstable and assumes an oscillatory mode. Dispersion of the surface layer increases at these pressures, resulting in a considerable burning-rate data scatter and an increase in the critical diameter of combustion.

At pressures above 10 MPa, gas-phase reactions start to play a considerable role, resulting in regaining the combustion stability. Combustion mechanism here differs strongly from that at low pressures. Burning rates at high pressures become lower than those might be expected from an extrapolation of the $r_b(p)$ dependence from low pressures to the high-pressure region. Assuming that the surface temperature in the interval of 10–20 MPa is still determined by the AN dissociation reaction, the degree to which ADN could decompose in the condensed phase would be unrealistically high, more than 100%. It is unlikely that increasing the pressure to 10 MPa can result in either change of ADN decomposition rate, reducing it by a factor of 10^2, or saturation of the surface-temperature growth. The latter case can happen when the dissociation/evaporation temperature reaches for its critical value, which probably takes place for AN dissociation at pressures about 20 MPa. At this pressure, many AN-based compositions revealed a change in their burning behavior.[45]

Therefore, a very specific combustion regime is presumably affected at pressures above 10 MPa: the burning rate is controlled by high-energy processes in the gas phase, while the low-energy but fast condensed-phase process plays a subordinate part and cannot propagate deep into the condensed material moving away from the supporting gaseous flame. As soon as the condensed-phase reaction front moves away from the gas reaction zone, its propagation stops because of heat withdrawal to dissociate/evaporate the substance at the surface.

Zeldovich showed[46] that failure of burning in gaseous systems as a result of heat losses from the reaction zone appeared when there was a RT_f^2/E decrease in the temperature of the zone T_f. A similar situation obviously takes place in combustion of systems with the leading reaction zone in the condensed phase. Because the relaxation time of processes occurring in the reaction zone is much less than the relaxation time of the preheated layer, the temperature gradient in the layer under the reaction zone is responsible for the steady-state burning. When ignited by an external heat source, the condensed phase is heated to a maximum achievable temperature, the AN dissociation temperature in this case. Because the self-heating in the condensed zone is insufficient to warm up the substance to this temperature, temperature in the reaction zone drops once the heat accumulated at ignition has been irreversibly consumed. The preheated layer has no time for readjustment, and combustion process in the condensed phase ceases. After a time, the gas flame reaches for the surface, inducing revival of the condensed-phase process, which propagates fast and then stops again.

The second section of the $r_b(p)$ curve is characterized by a decrease in the burning rate with pressure. The combustion velocity is still determined by the fast condensed-phase process, with the role of the gas phase reduced to igniting it after extinction. As the pressure grows and the surface temperature increases, the gas-phase process dominates over the condensed-phase combustion process and assumes total control over burning at pressures above 10 MPa.

The pressure exponent for the high-pressure portion of the $r_b(p)$ dependence is ~0.7, a value that usually points to a first-order leading reaction for the gas-phase combustion model. Such a reaction could be decomposition of the most reactive oxidizer in the gas phase, HNO_3, at temperature T_1 (1300–1400 K).

Decomposition of gaseous HNO_3 under shock-wave conditions in argon atmosphere is characterized by the decomposition rate constant, $k = 10^{6.2} \cdot (T)^{0.5} \cdot (47{,}300/RT)^8 \cdot \exp(-47{,}300/RT)$, $\mathrm{cm^3/mole \cdot s}$ (Ref. 47). Recalculation for the first-order reaction (argon concentration is $\sim 10^{-5}$ $\mathrm{mol/cm^3}$) at the average of the isothermal decomposition temperature interval gives $k = 10^{16.14} \cdot \exp(-47{,}300/RT)$, $\mathrm{s^{-1}}$.

Using a combustion model of volatile explosives[48] and assuming that decomposition of gaseous HNO_3 controls the burning rate, one can easily calculate the rate of burning:

$$\dot{m} = \sqrt{\frac{2\lambda\mu}{c_p(T_f - T_0)} \cdot \left(\frac{RT_f^2}{E}\right)^{a+1} \cdot \frac{a!}{(T_f - T_{01})^a} \cdot \left(\frac{\eta \cdot p}{RT_f}\right)^a \cdot A \exp\left(\frac{-E}{RT_f}\right)}$$

where the value of $T_{01} = T_0 - (L_m + L_{\mathrm{dis}})/c_p$ stands for the initial temperature T_0 with allowance for the heat consumed for melting L_m and dissociation L_{dis}.

The calculation of the burning rates on the assumption that the leading reaction is the HNO_3 decomposition one gives a good correspondence with experimental results at HNO_3 mole fraction in the gas taken as ~0.2 (assuming that 0.6 mole of ADN decomposes to AN and the rest decomposes to the two molecules of water and two molecules of N_2O) (Fig. 10).

Hence, the overall combustion mechanism of ADN comprises the fast decomposition in the melt, resulting in aerosol flow above the surface and slow reaction in the gas. The only difference in combustion within different pressure intervals lies in which of the reactions controls the process. The fast but energy-limited condensed-phase decomposition controls combustion at low pressures, has to accommodate itself to the slow but energy-rich heat-release process in the gas phase at middle pressures, and is incapable of controlling the burning rate at high pressures because of limited heat produced in it.

IV. Conclusions

Temperature measurements suggest a three-zone structure of the ADN flame. The ADN surface temperature corresponds to the temperature of dissociation of AN, a decomposition product of ADN in melt. Temperature just above the surface (the aerosol zone) is controlled first by the reaction of AN dissociation at the surface

of small droplets followed then by dissociation of remaining ADN droplets. The heat feedback from the gas to the surface is negligibly small. The first flame comprises reactions of NH_3 oxidation by nitric acid decomposition products. In the second flame, the complete thermodynamic heat release is attained.

The ADN combustion mechanism includes the fast decomposition reaction in the condensed phase to result in an aerosol flow above the surface and slow reactions in the gas. At low pressures, the decomposition reaction in the melt plays a dominant role. In the middle pressure interval, the fast but energy-limited heat-release process in the condensed phase has to adapt itself to the slow but energy-rich heat-release process in the gas phase. At high pressures (above 10 MPa), the condensed-phase decomposition reaction can no longer control combustion because of the lack of heat produced in it.

The ADN combustion can be satisfactorily described by a condensed-phase combustion model with the rate-controlling reaction being the ADN decomposition in the melt at low pressures (to 1 MPa) and a gas-phase model at high pressures (above 10 MPa), with the rate-controlling reaction being HNO_3 decomposition in the first flame.

Acknowledgment

The authors are most grateful to Woodward Waesche for the generous help in preparation of the paper.

References

[1]Pak, Z. P., "Some Ways to Higher Environmental Safety of Solid Rocket Propellant Application," AIAA Paper 93-1755, June 1993.

[2]Parr, T., and Hanson-Parr, D., "ADN Diffusion Flame Structure at Elevated Pressure," *Proceedings of the 30th JANNAF Combustion Subcommittee Meeting*, CPIA Pub. 606, Baltimore, MD, 1993, pp. 1–13.

[3]Russell, T. P., Stern, A. G., Koppes, W. M., and Bedford, C. D., "Thermal Decomposition and Stabilization of Ammonium Dinitramide," *Proceedings of the 29th JANNAF Combustion Subcommittee Meeting*, CPIA Pub. 593, Baltimore, MD, Vol. II, 1992, pp. 339–345.

[4]Brill, T. B., Brush, P. J., and Patil, D. G., "Thermal Decomposition of Energetic Materials 58. Chemistry of Ammonium Nitrate and Ammonium Dinitramide near the Burning Surface Temperature," *Combustion and Flame*, Vol. 92, Nos. 1-2, 1993, pp. 178–186.

[5]Manelis, G. B., "Thermal Decomposition of Dinitramide Ammonium Salt," *Proceedings of the 26th International Annual ICT Conference*, Paper 15, Fraunhofer ICT, Pfinztal, FRG, 1995, pp. 15-1–15-17.

[6]Vyazovkin, S., and Wight, C. A., "Ammonium Dinitramide: Kinetics and Mechanism of Thermal Decomposition," *Journal of Physical Chemistry A*, Vol. 101, No. 31, 1997, pp. 5653–5658.

[7]Vyazovkin, S., and Wight, C. A., "Thermal Decomposition of Ammonium Dinitramide at Moderate and High Temperatures," *Journal of Physical Chemistry A*, Vol. 101, No. 39, 1997, pp. 7217–7221.

[8]Gidaspov, B. V., Tzelinskii, I. V., and Shcherbinin, M. B., "Photolysis of Dinitramide Salts in Solutions," *Russian Journal of General Chemistry*, Vol. 67, No. 6, 1997, pp. 911–914.

[9]Oxley, J. C., Smith, J. L., Zheng, W., Rogers, E., and Coburn, M. D., "Thermal Decomposition Studies on Ammonium Dinitramide (ADN) and ^{15}N and ^{2}H Isotopomers," *Journal of Physical Chemistry A*, Vol. 101, No. 31, 1997, pp. 5646–5652.

[10]Kazakov, A. I., Rubtsov, Yu. I., Manelis, G. B., and Andrienko, L. P., "Kinetics of the Thermal Decomposition of Dinitramide. 1. The Decomposition of Different Forms of Dinitramide," *Russian Chemical Bulletin*, Vol. 46, No. 12, 1997, pp. 2015–2020.

[11]Kazakov, A. I., Rubtsov, Yu. I., Manelis, G. B., and Andrienko, L. P., "Kinetics of the Thermal Decomposition of Dinitramide. 2. Kinetics of the Interaction of Dinitramide with the Decomposition Products and other Components of a Solution," *Russian Chemical Bulletin*, Vol. 47, No. 1, 1998, pp. 39–44.

[12]Kazakov, A. I., Rubtsov, Yu. I., Andrienko, L. P., and Manelis, G. B., "Kinetics of the Thermal Decomposition of Dinitramide. 3. Kinetics of the Heat Release at ADN Thermolysis in the Liquid Phase," *Russian Chemical Bulletin*, Vol. 47, No. 3, 1998, pp. 379–384.

[13]Fetherolf, B. L., and Litzinger, T. A., "Physical and Chemical Processes Governing the CO_2 Laser-Induced Deflagration of Ammonium Dinitramide (ADN),"*Proceedings of the 29th JANNAF Combustion Subcommittee Meeting*, CPIA Pub. 593, Baltimore, MD, Vol. II, 1992, pp. 327–338.

[14]Fogelzang, A. E., Sinditskii, V. P., Egorshev, V. Y., Levshenkov, A. I., Serushkin, V. V., and Kolesov, V. I., "Combustion Behavior and Flame Structure of Ammonium Dinitramide," *Proceedings of the 28th International Annual Conference of ICT*, Paper 99, Fraunhofer ICT, Pfinztal, FRG, 1997, pp. 1–14.

[15]Denisiuk, A. P., Kuleshova, T. M., and Shepelev, Yu. G., "Combustion of Ammonium Dinitramide and Their Mixtures with Organic Fuels," *Doklady Akademii Nauk*, Vol. 368, No. 3, 1999, pp. 350–353 (in Russian).

[16]Strunin, V. A., D'yakov, A. P., and Manelis, G. B., "Combustion of Ammonium Dinitramide," *Combustion and Flame*, Vol. 117, No. 1–2, 1999, pp. 429–434.

[17]Atwood, A. I., Boggs, T. L., Curran, P. O., Parr, T. P., Hanson-Parr, D., Price, C. F., and Wiknich, J., "Burn Rate of Solid Propellant Ingradients, Part 1: Pressure and Initial Temperature Effects," *Journal of Propulsion and Power*, Vol. 15, No. 6, 1999, pp. 740–748.

[18]Zenin, A. A., Puchkov, V. M., and Finjakov, S. V., "Physics of ADN Combustion," AIAA Paper 1999-0595, Jan. 1999.

[19]Fetherolf, B. L., and Litzinger, T. A., "CO_2 Laser-Induced Combustion of Ammonium Dinitramide (ADN)," *Combustion and Flame*, Vol. 114, No. 3-4, 1998, pp. 515–530.

[20]Parr, T., and Hanson-Parr, D., "ADN Propellant Diffusion Flame Structure," *Proceedings of the 30th JANNAF Combustion Subcommittee Meeting*, CPIA Pub. 593, Baltimore, MD, Vol. II, 1992, pp. 313–328.

[21]Weiser, V., Eisenreich, N., Baier, A., and Eckl, W., "Burning Behavior of ADN Formulation," *Propellants, Explosives, Pyrotechnics*, Vol. 24, No. 3, 1999, pp. 163–167.

[22]Sinditskii, V. P., Fogelzang, A. E., Egorshev, V. Y., Levshenkov, A. I., Serushkin, V. V., and Kolesov, V. I., "Combustion Peculiarities of ADN and ADN-Based Mixtures," *Combustion of Energetic Materials*, edited by K. K. Kuo, and L. T. DeLuca, Begell House, New York, 2002, pp. 502–512.

[23]Korobeinichev, O. P., Paletsky, A. A., Tereshenko, A. G., and Volkov, E. N., "Study of Combustion Characteristics of Ammonium Dinitramide/Polycaprolactone Propellants," *Journal of Propulsion and Power*, Vol. 19, No. 2, 2003, pp. 203–212.

[24]Chakravarthy, S. R., Freeman, J. F., Price, E. W., and Sigman, R. K., "Combustion of Propellants with Ammonium Dinitramide," *Propellants, Explosives, Pyrotechnics*, Vol. 29, No. 4, 2004, pp. 220–230.

[25]Park, J., Chakraborty, D., and Lin, M. C., "Thermal Decomposition of Gaseous Ammonium Dinitramide at Low Pressure: Kinetic Modeling of Product Formation with ab initio MO/cVRRKM Calculations," *Proceedings of the 27th International Symposium on Combustion*, The Combustion Institute, Pittsburgh, PA, 1998, pp. 2351–2357.

[26]Korobeinichev, O. P., Kuibida, L. V., Paletsky, A. A., and Shmakov, A. G., "Combustion Chemistry of Energetic Materials Studied by Probing Mass Spectrometry," *Decomposition, Combustion and Detonation Chemistry of Energetic Materials*, edited by T. B. Brill, T. P. Russell, W. C. Tao, and R. B. Wardle, *Proceedings of MRS Symposium*, Vol. 418, MRS, Pittsburgh, PA, 1996, pp. 245–255.

[27]Korobeinichev, O. P., Kuibida, L. V., Paletsky, A. A., and Shmakov, A. G., "Molecular-Beam Mass-Spectrometry to Ammonium Dinitramide Combustion Chemistry Studies," *Journal of Propulsion and Power*, Vol. 14, No. 6, 1998, pp. 991–1000.

[28]Luk'yanov, O. A., Konnova, Y. V., Klimova, T. A., and Tartakovsky, V. A. "Dinitramide and Its Salts. 2. Dinitramide in Direct and Reverse Michael-Type Reactions," *Russian Chemical Bulletin*, Vol. 43, No. 7, 1994, pp. 1200–1202.

[29]Feick, G., "The Dissociation Pressure and Free Energy of Formation of Ammonium Nitrate," *Journal of American Chemical Society*, Vol. 76, No. 22, 1954, pp. 5858–5860.

[30]Manelis, G. B., Nazin, G. M., Rubtsov, Yu. I., and Strunin, V. A., *Thermal Decomposition and Combustion of Explosives and Propellants*, Nauka, Moscow, 1996, pp. 101–115 (in Russian).

[31]Russell, T. P., Piermarini, G. J., Block, S., and Miller, P. J., "Pressure, Temperature Reaction Phase Diagram for Ammonium Dinitramide," *Journal of Physical Chemistry A*, Vol. 100, No. 18, 1996, pp. 3248–3251.

[32]Pavlov, A. N., and Nazin, G. M., "Decomposition Mechanism of Dinitramide Onium Salts," *Russian Chemical Bulletin*, Vol. 46, No. 11, 1997, pp. 1848–1850.

[33]Tartakovsky, V. A., "The Design of Stable High Nitrogen System," *Decomposition, Combustion and Detonation Chemistry of Energetic Materials*, edited by T. B. Brill, T. P. Russell, W. C. Tao, and R. B. Wardle, *Proceedings of MRS Symposium*, Vol. 418, MRS, Pittsburgh, PA, 1996, pp. 15–24.

[34]Andreev, K. K., *Thermal Decomposition and Combustion of Explosives*, Nauka, Moscow, 1966, pp. 283–294 (in Russian).

[35]Strunin, V. A., and Manelis, G. B., "Analysis of Elementary Models for the Steady-State Combustion of Solid Propellants," *Journal of Propulsion and Power*, Vol. 11, No. 4, 1995, pp. 666–675.

[36]Shmakov, A. G., Korobeinichev, O. P., and Bol'shova T. A., "Thermal Decomposition of Ammonium Dinitramide Vapor in a Two-Temperature Flow Reactor," *Combustion, Explosion, and Shock Waves*, Vol. 38, No. 3, 2002, pp. 284–294.

[37]Inami, C. H., Rosser, W. A., and Wise, H., "Dissociation Pressure of NH_4ClO_4," *Journal of Physical Chemistry*, Vol. 67, No. 5, 1963, pp. 1077–1079.

[38]Stull, D. R., Westrum, E. F., and Sinke, G. C., *The Chemical Thermodynamics of Organic Compounds*, Wiley, New York, 1969.

[39]Mebel, A. M., Lin, M. C., Morokuma, K., and Melius, C. F., "Theoretical Study of the Gas-Phase Structure, Thermochemistry, and Decomposition Mechanisms of NH_4NO_2 and $NH_4N(NO_2)_2$," *Journal of Physical Chemistry*, Vol. 99, No. 18, 1995, pp. 6842–6848.

[40]Politzer, P., Seminario, J. M., and Concha, M. C., "Energetics of Ammonium Dinitramide Decomposition Steps," *Journal of Molecular Structure (Theochem)*, Vol. 427, No. 1-3, 1998, pp. 123–130.

[41]Goodwin, E. J., Howard, N. W., and Legon, A. C., "The Rotation Spectrum of ^{15}N-Ammonium Chloride Vapour: Characterization of Hydrogen-Bonded Dimer $H_3N...HCl$," *Chemical Physics Letters*, Vol. 131, No. 4–5, 1986, pp. 319–324.

[42]Ermolin, N. E., "Modeling of Pyrolysis of Ammonium Dinitramide Sublimation Products Under Low Pressure Conditions," *Combustion, Explosion, and Shock Waves*, Vol. 40, No. 1, 2004, pp. 92–109.

[43]Sinditskii, V. P., Egorshev, V. Y., Levshenkov, A. I., and Serushkin, V. V., "Combustion of Ammonium Dinitramide. Part 1: Burning Behavior," *Journal of Propulsion and Power*, Vol. 22, No. 4, 2006, pp. 769–776.

[44]Zeldovich, Y. B., "Theory of Combustion of Propellants and Explosives," *Zhurmal Eksperimentalnoy i Teoreticheskoi Fiziki (Russion Journal of Experimental and Theoretical Physics)*, Vol. 12, No. 11–12, 1942, pp. 498–524 (in Russian).

[45]Glazkova, A. P., *Catalysis of Explosive Combustion*, Nauka, Moscow, 1976, pp. 115–139 (in Russian).

[46]Zeldovich, Y. B., "Theory of Propagation Limit of Slow Flame," *Zhurnal Eksperimentalnoy i Teoreticheskoi Fiziki (Russion Journal of Experimental and Theoretical Physics)*, Vol. 11, No. 1, 1941, pp. 159–169 (in Russian).

[47]Harrison, H., Johnston, H. S., Hardwick, E. R., "Kinetics of the Thermal Decomposition of Nitric Acid Vapor. IV. A Shock Tube Study Between 800-1200 K," *Journal of the American Chemical Society*, Vol. 84, No. 13, 1962, pp. 2478–2483.

[48]Zeldovich, Y. B., and Frank-Kamenetskii, D. A., "The Theory of Thermal Propagation of a Flame," *Zhurnal Fizicheskoi Khimii (Russian Journal of Physical Chemistry)*, Vol. 12, No. 1, 1938, pp. 100–105 (in Russian).